Available online at www.sciencedirect.com

ScienceDirect

Proceedings of the Combustion Institute 38 (2021) 1737–1744

Proceedings of the Combustion Institute

www.elsevier.com/locate/proci

Detection of the keto-enol tautomerization in acetaldehyde, acetone, cyclohexanone, and methyl vinyl ketone with a novel VUV light source

David E. Couch [a], Quynh L.D. Nguyen [a], Allison Liu [a], Daniel D. Hickstein [b], Henry C. Kapteyn [a,b], Margaret M. Murnane [a], Nicole J. Labbe [c,*]

[a] *JILA, Department of Physics, University of Colorado Boulder and NIST, Boulder, CO, USA*
[b] *Kapteyn-Murnane Laboratories Inc. (KMLabs Inc.), 4775 Walnut St #102, Boulder, CO 80301, USA*
[c] *Department of Mechanical Engineering, University of Colorado Boulder, Boulder, CO 80309-0427, USA*

Received 7 November 2019; accepted 11 June 2020
Available online 9 September 2020

Abstract

The discovery of enols in combustion environments and our atmosphere has garnered increasing attention to the many unanswered questions surrounding enol chemistry. The scarcity of experimental data concerning these enols renders combustion and atmospheric models with a lack of constraining parameters, leading to varying computational predictions. Experimental detection is difficult because mass spectrometry, a powerful tool for probing a wide variety of species, cannot distinguish between enols and their thermodynamically favorable ketone isomers. A solution to this ambiguity is to use tunable vacuum ultraviolet (VUV) light from a synchrotron to identify the presence of the enol by its lower ionization energy compared to the isomer. We present a tabletop-scale VUV light source that implements highly cascaded harmonic generation, a new regime of cascaded nonlinear optics, to provide a set of spectral lines spaced by 1.2 eV. We demonstrate that the variety of photon energies available allows us to detect the keto-enol tautomerization of four aldehydes and ketones. By combining this novel VUV light source with an established microreactor, we first revisit the formation of vinyl alcohol from acetaldehyde and confirm that the observed isomerization is indeed unimolecular. Secondly, we observe the thermal tautomerization of acetone to propen-2-ol for the first time. Finally, we observe the thermal tautomerization of cyclohexanone to 1-cyclohexenol and methyl vinyl ketone to 2-hydroxybutadiene, where the results are in good agreement with those reported at a synchrotron. Our measurements can be used to constrain models, inform future experimental studies of enol reactivity, and potentially enhance current understanding of combustion and environmental chemistry.

Keywords: VUV light source; Keto-enol tautomerization; Isomer detection; Tabletop tunable VUV; Enol intermediates

* Corresponding author.
E-mail address: nicole.labbe@colorado.edu (N.J. Labbe).

https://doi.org/10.1016/j.proci.2020.06.139
1540-7489

1. Introduction

Since the discovery that enols are present in high concentrations in flames [1], the chemistry of enols has been heralded as important for understanding many gas-phase reacting systems. In addition to combustion, enols are thought to play a significant role in the atmosphere, possibly providing a source for tropospheric acid production [2–4]. Despite the identification of enols as key intermediates in combustion, many kinetic models do not include pathways to form enols, which may be due to the uncertainty of the chemistry behind their formation. Enols, the tautomers of aldehydes and ketones, can be produced in a variety of ways, where addition-elimination reactions have been suggested as major sources. For example, enols may be formed via OH-radical addition elimination reactions with alkenes [5,6] or through other fuel radical + flame radical reactions [7]. Of course, if saturated alcohols are present in a flame, they can also form enols via subsequent abstractions and β-scissions as well, as observed with various butanol isomers [8].

A perhaps more controversial source of enols is through direct gas-phase keto-enol tautomerization of ketones and aldehydes. Vasiliou et al. [9,10] was among the first to present experimental evidence of a direct gas-phase isomerization of acetaldehyde to vinyl alcohol through a keto-enol tautomerization, providing support using both photoionization mass spectrometry and infrared spectroscopy diagnostics with a pyrolysis microreactor. In fact, Vasiliou et al. [9,10] proposed that the keto-enol tautomerization was a major pathway for high temperature unimolecular decomposition of acetaldehyde, though at the time there were questions as to whether the observed vinyl alcohol was due to bimolecular chemistry rather than the keto-enol tautomerization. Sivaramakrishan et al. [11] conducted a combined theory and experimental study of acetaldehyde and determined that, in fact, the keto-enol tautomerization to vinyl alcohol was important. However, differences between the two studies [9,10] may be due to the presence of significant bimolecular chemistry in the microreactor work. Furthermore, understanding the extent to which the keto-enol tautomerization is active under combustion conditions could have consequences for predictions of other combustion intermediates, as subsequent reactions of the enol with other radicals present in the flame may change the final distribution of the predicted intermediate species pool.

Two of the challenges in determining the role of keto-enol tautomerization in combustion are highlighted in the acetaldehyde case. First, because both the keto and enol isomers have the same mass, a sensitive diagnostic is required to measure the enol directly. It was only when photoionization mass spectrometry was coupled to a tunable VUV light source via a synchrotron that it was possible to separate the enol intermediates in a flame from their aldehyde and ketone counterparts [1]. Secondly, to isolate the direct keto-enol tautomerization pathway, dilute conditions are required such that the chemistry is not clouded by subsequent bimolecular chemistry. At the University of Colorado Boulder, a recently developed tunable VUV light source [12] provides the opportunity to repeat the experiments of Vasiliou et al. [9,10] for a variety of aldehydes and ketones at less concentrated conditions to revisit the extent to which keto-enol tautomerizations are present under high temperature conditions. In this work, we study the thermal keto-enol isomerization of 4 species: acetaldehyde, acetone, cyclohexanone, and methyl vinyl ketone. We report the first known observation of thermal isomerization of acetone to propen-2-ol. We additionally provide observations of the isomerization of acetaldehyde to vinyl alcohol, cyclohexanone to 1-cyclohexenol, and methyl vinyl ketone to 2-hydroxybutadiene.

2. Experimental work

Pyrolysis microreactor: For this work, we use a pyrolysis microreactor in conjunction with photoionization mass spectrometry detection techniques described in detail previously [10,13]. Of note, we now use a continuous flow through the reactor at CU Boulder as has been done previously at synchrotron user facilities [14]. A brief description specific to our setup for this work is given here and highlighted in Fig. 1. A reactant mixture (typically a small concentration, 0.01–1%, of a fuel in a helium carrier gas) is fed to the microreactor through a mass flow controller (MKS) at a total flow of ~200 sccm. The pressure in the line leading from the reactant mixture vessel to the reactor is generally 350–500 torr, rising as the temperature of the reactor rises due to the increasing viscosity of the helium carrier gas. The mixture flows through a 40 μm aperture immediately before entering the microreactor. The microreactor itself consists of a straight silicon carbide tube (28 mm long, 1 mm ID, 1.8 mm OD), with no aperture at the exit and is resistively heated to temperatures of 800–1600 K. Flow simulations of the reactor [15] indicate a residence time of ~60 μs in the reactor under these conditions.

The reactor is heated resistively by running a current (around 5 A) through the SiC itself. The wires from the power supply connect to molybdenum holders which hold graphite disks that fit snugly on the exterior of the reactor. The distance between disks is about 8 mm, ending about 2 mm from the exit of the reactor. The heat source is placed close to the end of the reactor to avoid damaging the base plate that holds the reactor base and the thermocouple and power wiring. The temperature is measured on a type C thermocouple (K-Re

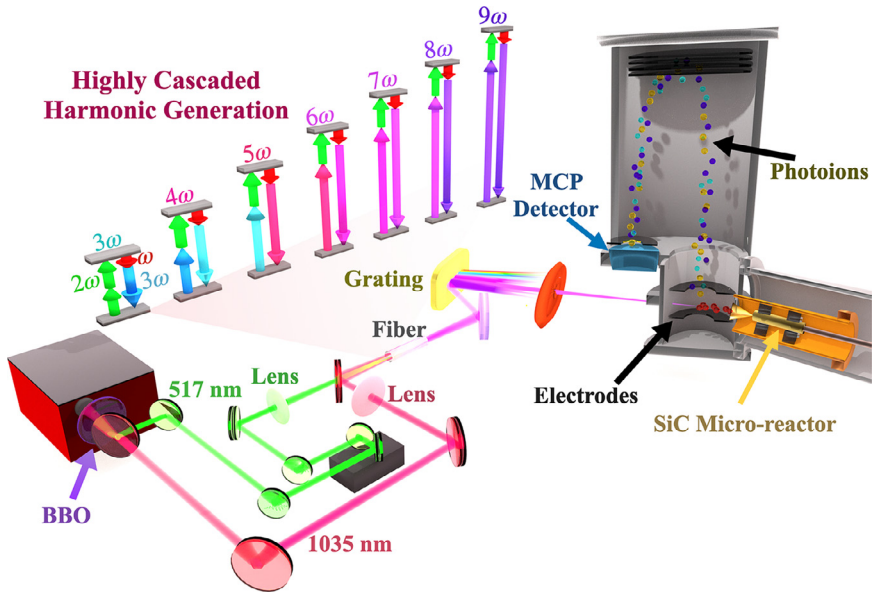

Fig. 1. Experimental setup. Two wavelengths generated by a ytterbium-doped fiber laser are combined in a xenon-filled hollow negative-curvature fiber to generate a variety of VUV spectral lines spaced by 1.2 eV. One of several possible routes for the cascaded four-wave mixing is illustrated. A single spectral line is selected by a grating monochromator and used to ionize a supersonic jet expanding out of a SiC microreactor held at a temperature of 300–1500 K. Ions pass through a reflectron mass spectrometer to an MCP detector.

alloy) spot welded to thin tantalum foil, which is tied to the reactor between the two graphite disks with tantalum wire. All materials in contact with the reactor were chosen to withstand temperatures of up to 1600 K.

The supersonic expansion of the gas mixture as it exits the tube cools the mixture, suppressing any further chemistry. A 200 μm skimmer about 1 cm from the exit of the reactor passes a small amount of the ejected gas into the ionization chamber. The remainder of the gas is collected by a turbomolecular pump (Pfeiffer TPU 1201 P) backed by a scroll pump (Agilent TriScroll 600). We observe a pressure of $\sim 5 \times 10^{-4}$ Torr in the source chamber and $\sim 8 \times 10^{-7}$ Torr in the ionization chamber under these conditions. Pressures in the continuous microreactor are roughly 50 Torr. The spectra obtained in this work are included as Supplemental Material.

Computational fluid dynamics simulations [15] have found that the microreactors are complex, non-linear devices. Chemical reactions in the microreactors vary exponentially with the gas temperature (which is rising) and quadratically with the pressure (which is falling). Prior work [15] has suggested that there is a small volume ("sweet-spot") in which most chemical reactions occur. The size and location of the "sweet-spot" can vary strongly with changes in the mass flowrate, reactor dimensions (diameter, length), material (SiC, quartz, or Al_2O_3), and the nature of the buffer gas (He, Ne, Ar).

KMLabs VUV light source: The ionization source for the photoionization mass spectrometry diagnostics used in this work was a pre-production prototype of the KMLabs Hyperion VUV(TM), that uses an ultrafast fiber laser source in conjunction with highly-cascaded four-wave-mixing harmonic generation in a xenon-filled hollow negative-curvature fiber [12]. This harmonic generation process is described in detail elsewhere [16], so we provide a brief description here. The output of a ytterbium-doped fiber modelocked oscillator is amplified in 3 stages by chirped-pulse amplification. This results in approximately 10 W average power at a center wavelength of 1035 nm, 1 MHz repetition rate, and 160 fs pulse duration. We use a β-BBO crystal to generate 4 W (4 μJ pulse energy) of the second harmonic, 517 nm, and focus both the 517 nm and 1035 nm light into a hollow-core negative curvature fused silica fiber. The two-color driving laser enables a cascaded four-wave-mixing process [17] that generates all harmonics of the 1035 nm fundamental up to the 15th harmonic. For this work, we use the 7th harmonic (8.4 eV, 6×10^{12} photons/s), 8th harmonic (9.6 eV, 3×10^{12} photons/s), and 9th harmonic (10.8 eV, 4×10^{11} photons/s).

The VUV generated in the fiber is spectrally separated and focused onto the target gas jet using an

in-vacuum folded Wadsworth monochromator. For this experiment, the monochromator consists of a flat custom-coated rejector mirror, a spherical focusing mirror, a flat diffraction grating, and a 1 mm exit slit. The rejector mirror is a 2″ diameter fused silica window mounted near grazing angle, coated to transmit 99% of the 1035 nm, 517 nm, and 345 nm light while reflecting >90% of all shorter wavelengths. The focusing mirror is a 1″ diameter, $R = 400$ mm spherical MgF_2-coated aluminum concave mirror. The diffraction grating is blazed for 120 nm with 600 grooves/mm (33021FL01–100R, Newport Richardson), recoated with MgF_2-coated aluminum. We use no optics between the exit slit and the gas jet with the exception of a MgF_2 window to prohibit xenon flowing from the monochromator into the ionization chamber. This window absorbs about 70% of the 10.8 eV photons and all photons of higher energy.

Pulsed ion extraction: For this experiment, we must reduce the effective repetition rate of the experiment by pulsing the voltages on the ion optics in the ionization chamber. Immediately below the ionization region (the overlap between the gas jet and the VUV light), a repeller charged to around 1500 V repels ions upward, and an extractor charged to around 700 V lies immediately above the ionization region. A mesh-covered hole in the extractor allows the ions to pass through into an acceleration region, which ends at a grounded mesh-covered plate. The ions then pass through an ion reflector before reaching a timing multichannel plate (MCP). Under ordinary operation, the time between the laser pulse and the ion detection on the MCP is used to calculate the mass of the ion. However, our laser generates pulses at a repetition rate of 1 MHz, while the ion flight times are typically 30 μs. With the repeller and extractor always charged to operational voltage, we would observe every signal peak copied every 1 μs. With 5–10 species present during each pyrolysis experiment, the density of peaks would severely impede interpretation. Instead, we pulse the voltage on the repeller with a repetition rate of 10 kHz, corresponding to a 100 μs delay between pulses. We use a commercial high voltage switch (Behlke HTS 21–03-GSM) with a home-built circuit to switch the repeller voltage. Ions take approximately 2 μs to drift out of the extractable region, so each voltage pulse extracts ions produced during the previous 2–3 laser pulses. Thus, the current setup only extracts 2–3% of the ions produced (1000,000 Hz/10,000 Hz = 100 VUV pulses per voltage pulse). More efficient ion detection, as demonstrated by mass spectrometers optimized for use at quasi-continuous synchrotrons [18], could increase count rates by more than an order of magnitude. The time between the voltage pulse and the signal on the MCP is used to calculate the mass of the ion, disregarding the exact timing of the laser pulses. The precise timing of the brief voltage pulse (2 ns) from the MCP during an ion detection event is recorded by a high-speed digitizer (Acqiris U1084A-001) using the Acqiris PeakTDC software. The mass resolution of this instrument is about m/Δm=750 (FWHM).

Comparison to other light sources: This tabletop VUV light source provides a valuable middle ground between synchrotron user-facilities that are shared amongst many research teams and single-spectral-line VUV sources that rely on an atomic resonance to aid the UV conversion. Access to multiple spectral lines is highly desirable for identifying isomers and reducing dissociative ionization. Compared to a synchrotron, the primary advantage of our source is size and availability. Additionally, the lower repetition rate of our source (1 MHz) allows the ions to pass completely out of the extracting region and the voltages to reset between consecutive VUV pulses, unlike at high repetition rate synchrotrons. Both instruments currently rely on pulsed ion extraction, but with a reduction of repetition rate to 100 kHz the voltage pulsing could be eliminated. Furthermore, the VUV generated from laser upconversion has a tighter focal spot, allowing more compact monochromators and potentially better mass resolution.

Isomerization may also be observed by light detection methods (e.g. IR absorption, laser induced fluorescence, Raman spectroscopies, or microwave spectroscopy). While powerful, each technique has its own disadvantages. In particular, all light detection methods generally suffer from poor sensitivity to species at very low concentrations, with a few notable exceptions. Additionally, these methods require some previous knowledge about the spectra of both target isomers or a close comparison with high-level theory.

Gas sample preparation: We used four chemicals for this work: cyclohexanone (Sigma Aldrich, >99% purity), acetone (Macron Fine Chemicals, >99.5% purity), acetaldehyde (Sigma Aldrich, >99.5% purity), and methyl vinyl ketone (a.k.a. 3-buten-2-one, Sigma Aldrich, 99% pure with 0.5% hydroquinone and 0.1% acetic acid). No further purification was performed. Each sample was degassed by two freeze-pump-thaw cycles to eliminate dissolved air. Dilutions were made by filling an empty chamber with a low pressure of sample (about 3 Torr), then with a high pressure of helium carrier gas (about 3000 Torr). Sample concentrations ranged from 0.01% to 2% (error = 0.1 x concentration + 0.01%).

3. Results and discussion

Acetaldehyde to Vinyl Alcohol Isomerization: Acetaldehyde has the most widely studied direct keto-enol tautomerizion of our four reactants. As discussed earlier, Vasiliou et al. [9] experimentally detected evidence of the keto-enol

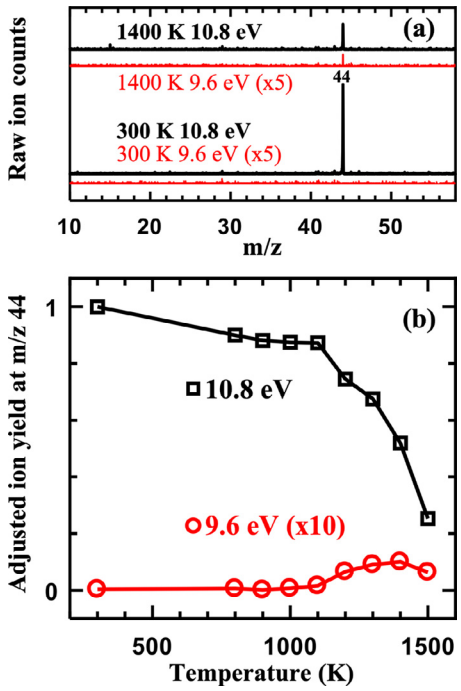

Fig. 2. Mass spectra of acetaldehyde thermal decomposition with varying temperature and photon energy. (a) At 300 K, acetaldehyde (IE 10.23 eV [20]) is only observed with 10.8 eV photons. At 1400 K, a small m/z 44 signal with 9.6 eV (red) reveals isomerization to vinyl alcohol (IE 9.3 eV for the dominant conformer [19]). (b) The observed ion yield, adjusted for photon flux and temperature-dependent jet sampling, shows the creation of vinyl alcohol at 1200 K and higher.

tautomerization to vinyl alcohol. However, given the 1% concentrations of acetaldehyde in the reaction sample, questions arose whether the source of the observed vinyl alcohol was either wall or bimolecular reactions. In their follow up paper [10], concentrations were reduced to 0.1% and the photoionization mass spectrometry experiments were repeated, both with pulsed flow at CU Boulder and with continuous flow at the Advanced Light Source. The possibility of bimolecular reactions was not ruled out for the pulsed flow experiments at CU Boulder; however, clear evidence of some vinyl alcohol was also seen in the photoionization efficiency scans. Though Sivaramakrishnan et al. [11] were blind to the enol in their H/D-ARAS experiments, their model derived from theory suggested that at short time scales (<150 μs) some vinyl alcohol would be present. This is further supported by another theoretical work [4].

We studied the isomerization of acetaldehyde to vinyl alcohol at elevated temperatures in our continuous microreactor experiment, shown in Fig. 2. The products of a heated mixture of 0.1% acetaldehyde in helium were ionized by two different photon energies: 9.6 eV photons to ionize only vinyl alcohol (measured IE 9.30 eV [19]) and 10.8 eV photons which can ionize both vinyl alcohol and acetaldehyde (measured IE 10.2295 eV [20]). A signal appears at m/z 44 using 9.6 eV photons for temperatures of 1100–1500 K. Since 9.6 eV is well below the ionization threshold for acetaldehyde, this signal indicates the presence of vinyl alcohol in small concentrations. While our results are presented qualitatively, an estimate of our observed tautomerization efficiency is consistent with that predicted by Sivaramakrishnan et al. [11] within our estimated error of a factor of 3 (see Supplemental Material). The small drop in acetaldehyde signal at 800–1100 K could be caused by a local hot spot on the reactor, or this drop could be an artifact caused by changing flow conditions as the reactor heats up. The Supplemental Material describes our method for converting raw ion counts into adjusted ion yield by correcting for photon flux and changes in jet sampling. At temperatures above 1300 K, thermal decomposition of both acetaldehyde and vinyl alcohol substantially deplete the total signal. Products CH_3 (m/z 15) and HCO (m/z 29) of the decomposition of acetaldehyde can be observed at a low level, but other products H and CO from acetaldehyde, as well as C_2H_2, H_2O, H, and OH from vinyl alcohol cannot be ionized due to a MgF_2 window in the beam path absorbing photons above 11 eV.

At 0.1% fuel concentrations, questions about whether the observed vinyl alcohol is indeed a unimolecular product remains. In order to check for bimolecular influences on isomerization, we studied the pyrolysis of acetaldehyde at 3 concentrations: 0.1%, 0.5%, and 2%. We observe a strong concentration dependence of ketene (CH_2=C=O, m/z 42) and ethylene (CH_2=CH_2, m/z 28), both known bimolecular products. The most likely pathway for the formation of ketene is hydrogen abstraction from acetaldehyde by methyl radicals produced by dissociation, followed by β-scission to form ketene (Eq. (1)). The formation of ethylene has been the subject of debate. Schuchmann and Laidler [21] proposed that the source of ethylene in their studies was due to an addition-elimination reaction between H-atom and vinyl alcohol (Eq. (2)), while Bardi and Marta [22] proposed it was instead from an addition-elimination reaction between H-atom and acetaldehyde itself (Eq. (3)).

$$CH_3CHO + CH_3 \rightarrow (CH_3CO \text{ or } CH_2CHO) + CH_4 \rightarrow CH_2CO \quad (1)$$

$$CH_2CHOH + H \rightarrow (CH_2CH_2OH) \rightarrow OH + C_2H_4 \quad (2)$$

$$CH_3CHO + H \rightarrow (CH_3CH_2O) \rightarrow OH + C_2H_4 \quad (3)$$

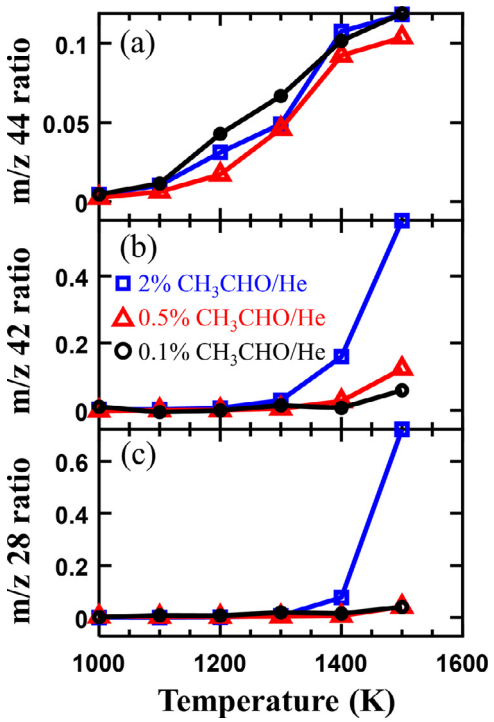

Fig. 3. The ratio of ion count corresponding to (a) vinyl alcohol, (b) ketene, and (c) ethylene to the ion count associated with acetaldehyde for varying concentration of acetaldehyde in helium. The total ion count at m/z 44 using 10.8 eV photons is used as the acetaldehyde count for comparison in all three panels, though we note that some of these counts actually arise from ionization of vinyl alcohol. Vinyl alcohol shows very little concentration dependence, indicating that at these conditions isomerization to vinyl alcohol is not substantially impeded or enhanced by chemical reactions. Both ketene and ethylene, known bimolecular products of acetaldehyde, show little production for ≤0.5% reactant concentrations.

At 2% concentration and 1500 K temperature, the ketene and ethylene signals were among the strongest peaks on the mass spectrum (Fig. S4). As concentrations are lowered, the signals for ethylene and ketene deplete significantly (Fig. 3). Despite the presence of this bimolecular chemistry, the relative concentrations of vinyl alcohol and acetaldehyde were unchanged. This supports that the vinyl alcohol is truly a unimolecular product rather than the result of bimolecular chemistry under our continuous reactor conditions.

Acetone to Propen-2-ol Isomerization: Acetone also shows clear evidence of isomerization to propen-2-ol at elevated temperatures. While it has been suggested that acetone can also isomerize to an enol (propen-2-ol [23]) and the keto-enol tautomerization has been induced by UV photoabsorption previously [24], we believe this is the first direct observation of thermal isomerization

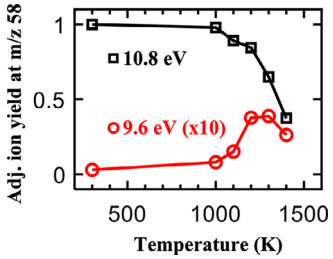

Fig. 4. Isomerization of acetone (IE 9.708 eV [25]) to propen-2-ol (IE 8.67 eV [26]) is observed by ionization with 9.6 eV photons. Both isomers are ionized by 10.8 eV photons for comparison. Ion yield is adjusted to compensate for photon flux and temperature-dependent flow conditions.

of acetone to its enol. In Fig. 4, the m/z=58 signal at 9.6 eV is first observed at ~1000 K. This is consistent with the observed enol in the acetaldehyde experiments, which are expected to have similar kinetics to acetone. The observed ion count has been corrected for drifting photon flux levels and changing flow conditions which modify the amount of the gas jet passing through the skimmer into the ionization chamber.

Notably, some of the ions observed with 9.6 eV could be ionized from vibrationally excited acetone, since the ionization energy of acetone at 9.71 eV is only 0.1 eV higher than the center of the 9.6 eV spectral line. The small signal at room temperature is attributed to a very small fraction of the bandwidth above 9.71 eV. However, we believe that most of the 9.6 eV signal arises from propen-2-ol, primarily due to previous evidence that the supersonic jet out of the reactor cools the jet effectively. Additionally, the temperature dependence of the observed 9.6 eV signal matches that expected from a Boltzmann distribution for isomerization but does not match that expected for 0.1–0.2 eV vibrational excitations of acetone.

Cyclohexanone to 1-Cyclohexenol Isomerization: As previously shown by Porterfield et al. [27] 1-cyclohexenol (IE 8.2 eV [27]) can be ionized by either 9.6 eV or 8.4 eV, while cyclohexanone (IE 9.16 eV [28]) can be ionized only by 9.6 eV. Their work utilized a similar setup to Vasiliou et al. [10], though all measurements were performed under continuous flow using synchrotron VUV light. Porterfield et al. [27] observed 1-cyclohexenol in a photoionization energy scan, with an appearance at 8.2 eV. This is further supported by a theoretical study on cyclohexanone unimolecular decomposition [29] where 1-cyclohexenol was the lowest molecular decomposition pathway. Our experiments with cyclohexanone also show clear evidence of isomerization to 1-cyclohexenol at elevated temperatures, which is shown in Fig. 5. We directly measured the enol concentration using 8.4 eV photons. The concentration is observed to

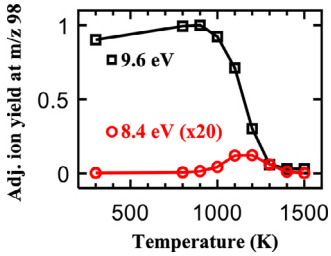

Fig. 5. Isomerization of cyclohexanone (IE 9.16 eV [28]) to 1-cyclohexenol (IE 8.2 eV [27]) is observed by ionizing with 8.4 eV photons. Both isomers are ionized by 9.6 eV for comparison.

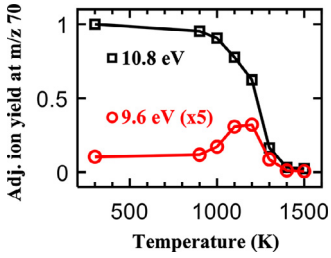

Fig. 6. Isomerization of methyl vinyl ketone (IE 9.66 eV [30]) to its isomer 2-hydroxybutadiene (IE 8.68 eV [31]) is observed by ionization with 9.6 eV photons. Both isomers are ionized by 10.8 eV for comparison. Since the bandwidth of the 9.6 eV spectral line extends beyond the ionization energy of methyl vinyl ketone at 9.66 eV, some ions are observed even at room temperature at 9.6 eV.

be highest for 1100–1200 K, and both isomers show thermal decomposition at higher temperatures. Again, the observed ion count has been corrected for drifting photon flux levels and changing flow conditions, which modify the amount of mixture passing through the skimmer into the ionization chamber. The slight rise in apparent concentration at 800–1000 K is attributed to a mismatch between the helium pressure in the ionization chamber, used in the calculation for adjusted ion yield, and the actual amount of cyclohexanone passing through the skimmer.

Methyl Vinyl Ketone to 2-Hydroxybutadiene Isomerization: The isomerization of methyl vinyl ketone to 2-hydroxybutadiene, shown in Fig. 6, was also observed by Porterfield et al. [27] Their interest in methyl vinyl ketone was rooted in the fact that it is a direct decomposition product of cyclohexanone. They observed the keto-enol tautomerization for methyl vinyl ketone (IE 9.66 ± 0.05 eV [30]) to 2-hydroxybutadiene (IE 8.68 eV [31]) through a photoionization efficiency scan at m/z 70 and observed ions at 1200 K appearing at ~8.7 eV. We repeat this measurement with only two photon energies, where 2-hydroxybutadiene can be ionized by 9.6 or 10.8 eV photons while methyl vinyl ketone cannot be ionized by 9.6 eV photons. Our results are consistent with previous results, with a small shift toward lower temperatures likely caused by slight differences in the reactor and thermocouple dimensions. The only theoretical study [32] known to the authors at the time of publication on methyl vinyl ketone, which identifies the keto-enol tautomerization, was on the photo-induced isomerization of methyl vinyl ketone.

Our ultrafast VUV light source has about 0.05 eV bandwidth at each spectral line, so a small amount of light just above the threshold of 9.66 ± 0.05 eV [30] passes through the monochromator during our 9.6 eV experiment. With the extra bandwidth, we are able to observe a small signal at m/z 70 at 300 K and 900 K with 9.6 eV photons. As with acetone, the temperature dependence of the 9.6 eV signal at m/z 70 for 1100–1300 K strongly resembles that expected for isomerization, not that expected for vibrational excitations of methyl vinyl ketone, so we attribute the additional signal at these temperatures to the presence of 2-hydroxybutadiene.

4. Conclusions

This work demonstrates the observation of a variety of gas-phase keto-enol tautomerizations using a microreactor coupled with photoionization mass spectrometry diagnostics. Uniquely, this experiment utilized a pre-production prototype of the KMLabs Hyperion VUV^{TM}, which allowed us to make use of the 7th harmonic (8.4 eV, 6×10^{12} photons/s), 8th harmonic (9.6 eV, 3×10^{12} photons/s), and 9th harmonic (10.8 eV, 4×10^{11} photons/s) to generate photons at various fixed wavelengths. In particular, the separation of the bands allowed us to detect differences in keto and enol isomers to directly detect the unimolecular pathway for the isomerization in-house at CU Boulder. Our work confirmed prior work on the keto-enol tautomerization between acetaldehyde and vinyl alcohol and supported previous work observing similar keto-enol tautomerizations in cyclohexanone and methyl vinyl ketone pyrolysis. Furthermore, we report the first experimental evidence of the theoretically suggested keto-enol tautomerization for acetone. The production of enols in combustion could have significant impact on models predicting combustion intermediates, since bimolecular pathways involving the enols could produce different subsequent products than the parent aldehydes and ketones. Finally, a concentration study with acetaldehyde was conducted to demonstrate that the observed enols are in fact due to unimolecular pathways. This work demonstrates the power of tabletop tunable VUV light sources for combustion research.

Declaration of Competing Interest

HCK and MMM have a financial interest in KMLabs Inc., which supplied a prototype laser for evaluation. D. Hickstein is an employee of KMLabs Inc.

Acknowledgements

KMLabs loaned the VUV light source for this work. Interfacing the VUV light source with the existing PIMS setup was supported by the DOE office of basic energy sciences (AMOS program) grant DE-FG02-99ER14982. D.E.C and Q.L.N acknowledge support from the NSF GRFP grants DGE-1650115 and DGE-1144083. N.J.L acknowledges support from the grant DE-SC0018627 funded by the U.S. Department of Energy, Office of Science. We gratefully acknowledge the assistance of G. Barney Ellison in this work.

Supplementary materials

Supplementary material associated with this article can be found, in the online version, at doi:10.1016/j.proci.2020.06.139.

References

[1] C.A. Taatjes, N. Hansen, A. McIlroy, J.A. Miller, J.P. Senosiain, S.J. Klippenstein, F. Qi, L. Sheng, Y. Zhang, T.A. Cool, J. Wang, P.R. Westmoreland, M.E. Law, T. Kasper, K. Kohse-Höinghaus, *Science* 308 (2005) 1887–1889.
[2] D.U. Andrews, B.R. Heazlewood, A.T. Maccarone, T. Conroy, R.J. Payne, M.J.T. Jordan, S.H. Kable, *Science* 33 (2012) 1203–1206.
[3] M.F. Shaw, B. Sztáray, L.K. Whalley, D.E. Heard, D.B. Millet, M.J.T. Jordan, D.L. Osborn, S.H. Kable, *Nat. Comm.* 9 (2018) 2584.
[4] M. Monge-Palacios, E. Grajales-Gonzáles, S.M. Sarathy, *Int. J. Quantum Chem.* 119 (2019) 25954.
[5] C.A. Taatjes, N. Hansen, J.A. Miller, T.A. Cool, J. Wang, P.R. Westmoreland, M.E. Law, T. Kasper, K. Kohse-Höinghaus, *J. Phys. Chem. A* 110 (2006) 3254–3260.
[6] G. Meloni, T.M. Selby, D.L. Osborn, C.A. Taatjes, *J. Phys. Chem. A* 112 (2008) 13444–13451.
[7] N.J. Labbe, R. Sivaramakrishnan, S.J. Klippenstein, *Proc. Combust. Inst.* 35 (2015) 447–455.
[8] K. Yasunaga, T. Mikajiri, S.M. Sarathy, T. Koike, F. Gillespie, T. Nagy, J.M. Simmie, H.J. Curran, *Combust. Flame* 159 (2012) 2009–2027.
[9] A.K. Vasiliou, K.M. Piech, X. Zhang, M.R. Nimlos, M. Ahmed, A. Golan, O. Kostko, D.L. Osborn, J.W. Daily, J.F. Stanton, G.B. Ellison, *J. Chem. Phys.* 135 (2011) 014306.
[10] A.K. Vasiliou, K.M. Piech, B. Reed, X. Zhang, M.R. Nimlos, M. Ahmed, A. Golan, O. Kostko, D.L. Osborn, D.E. David, K.N. Urness, J.W. Daily, J.F. Stanton, G.B. Ellison, *J. Chem. Phys.* 137 (2012) 164308.
[11] R. Sivaramakrishnan, J.V. Michael, L.B. Harding, S.J. Klippenstein, *J. Phys. Chem. A* 119 (2015) 7724–7733.
[12] J. Ramirez, D. Hickstein, D. Couch, M. Kirchner, M. Murnane, H. Kapteyn, S. Backus, in: Proceedings of the Conference on Lasers and Electro-Optics, San Jose, California, May 2019 (10.1364/CLEO_AT.2019.JM3E.4).
[13] X. Zhang, A.V. Friderichsen, S. Nandi, G.B. Ellison, D.E. David, J.T. McKinnon, T.G. Lindeman, D.C. Dayton, M.R. Nimlos, *Rev. Sci. Instrum.* 74 (2003) 3077–3086.
[14] T.K. Ormond, A.M. Scheer, M.R. Nimlos, D.J. Robichaud, T.P. Troy, M. Ahmed, J.W. Daily, T.L. Nguyen, J.F. Stanton, G.B. Ellison, *J. Phys. Chem. A* 119 (2015) 722–7234.
[15] Q. Guan, K.N. Urness, T.K. Ormond, D.E. David, G. Barney Ellison, J.W. Daily, *Int. Rev. Phys. Chem.* 33 (2014) 447–487.
[16] D.E. Couch, D.D. Hickstein, D.G. Winters, S.J. Backus, M.S. Kirchner, S.R. Domingue, J.J. Ramirez, C.G. Durfee, M.M. Murnane, H.C. Kapteyn, *Optica* 7 (2020) 832–837.
[17] C.G. Durfee, L. Misoguti, S. Backus, H.C. Kapteyn, M.M. Murnane, *J. Opt. Soc. Am. B* 19 (2002) 822–831.
[18] L. Sheps, I. Antonov, K. Au, *J. Phys. Chem. A* 123 (2019) 10804–10814.
[19] G.Y. Matti, O.I. Osman, J.E. Upham, R.J. Suffolk, H.W. Kroto, *J. Electron Spectrosc. Relat. Phenom.* 49 (1989) 195–201.
[20] D.J. Knowles, A.J.C. Nicholson, *J. Chem. Phys.* 60 (1974) 1180–1181.
[21] H.-.P. Schuchmann, K.J. Laidler, *Can. J. Chem.* 48 (1970) 2315–2319.
[22] I. Bardi, F. Marta, *Acta. Phys. Chem.* 19 (1973) 227–244.
[23] V. Saheb, M. Zokaie, *J. Phys. Chem. A* 122 (2018) 5895–5904.
[24] M.F. Shaw, D.L. Osborn, M.J.T. Jordan, S.H. Kable, *J. Phys. Chem. A* 121 (2017) 3679–3688.
[25] R.T. Wiedmann, L. Goodman, M.G. White, *Chem. Phys. Lett.* 293 (1998) 391–396.
[26] F. Turecek, Z. Havlas, *J. Org. Chem.* 51 (1986) 4066–4067.
[27] J.P. Porterfield, T.L. Nguyen, J.H. Baraban, G.T. Buckingham, T.P. Troy, O. Kostko, M. Ahmed, J.F. Stanton, J.W. Daily, G.B. Ellison, *J. Phys. Chem. A* 119 (2015) 12635–12647.
[28] B.J. Cocksey, J.H.D. Eland, C.J. Danby, *J. Chem. Soc. B Phys. Org.* 790 (1971) 790–792.
[29] A.M. Zaras, P. Dagaut, Z. Serinyel, *J. Phys. Chem. A* 119 (2015) 7138–7144.
[30] P. Masclet, G. Mouvier, *Relat. Phenom* 14 (1978) 77–97.
[31] F. Tureček, *Tetrahedron. Lett.* 25 (1984) 5133–5134.
[32] S. So, U. Wille, G. da Silva, *ACS Earth Space Chem.* 2 (2018) 753–763.